LIQUID–GAS PHASE TRANSITION IN FINITE NUCLEI WITHIN FERMIONIC MOLECULAR DYNAMICS

HANS FELDMEIER
Gesellschaft für Schwerionenforschung mbH
D-64220 Darmstadt

AND

JÜRGEN SCHNACK
Universität Osnabrück, Fachbereich Physik
Barbarastr. 7, D-49069 Osnabrück

1. Introduction

The liquid–gas phase transition of nuclear matter is presently investigated experimentally in several laboratories [1]. The task is very difficult because one can manipulate only finite nuclei and the measured information on the system is rather indirect. The difference to macro–physics is not only the smallness of the system with only about 200 constituents but also that one cannot control the thermodynamic quantities volume or pressure. The reason is that one is colliding two nuclei in order to produce excitation energy and compression. But as there is no container the system begins to expand into the vacuum right after the compression and heating phase. Therefore one is all the time in a transient state where equilibrium in its original meaning, namely a time–independent stationary macro state, is not reached.

The excitation energy of the nuclear system can be deduced by measuring all energies of the outgoing particles and clusters. Also the number of nucleons which belong to the nuclear system under investigation is fairly well known. In peripheral collisions the so called spectator matter, which is heated by ablation and participant nucleons which enter the spectator, moves with a speed close to the beam velocity and can thus be separated from participant matter. The excited spectator pieces are assumed to have little compression.

Central collisions lead to higher excitations and more compression. Selection of events with high transverse energies of the outgoing fragments are considered to be most central and are thus distinguished from more peripheral collisions. But there is always a certain amount of matter emitted in the forward backward direction which originates from the corona. Due to compression and heating the participant matter will develop a radial collective flow which obstructs equilibration. It is however possible to estimate its magnitude by assuming local equilibrium and a flow velocity profile, for example proportional to the distance from the center of the source.

A "freeze–out" concept is entering all considerations. Usually the time interval in which the collisions between the nucleons and the fragments cease is believed to be short enough so that global thermodynamic properties like temperature and flow velocity are frozen in. This allows to infer from the mean kinetic energies of the fragments the division into collective and thermal energy. The argument is that the thermal part of the center of mass motion is proportional to the temperature and independent on mass while the collective part is proportional to the mass. Both, measurements and molecular dynamics calculations support this picture.

Despite all these difficulties the hope is that multifragmention reactions will give information on the coexistence phase because at freeze–out several fragments coexist with vapor. The gas phase should be related to vaporization events which consist mainly of nucleons and only a few small clusters, while evaporating compound nuclei should represent the hot liquid.

The challenge to measure nuclear equations of state has been accepted not only for astrophysical reasons, like supernova explosions or neutron stars, but also because the subject in itself is of interest as one is dealing with a small charged Fermi liquid which is self–bound by the strong interaction.

2. Theoretical Approaches

Different from experiment a theoretical treatment can impose thermodynamic conditions like volume and temperature. Grand canonical mean–field calculations have been performed since long, both relativistic and non-relativistic, e.g. [2, 3, 4, 5, 6]. There are however two major shortcomings with that. First, a mean–field picture does not treat the coexistence region properly, fluctuations are missing and a Maxwell construction is needed. Second, they cannot describe the experimental non–equilibrium situation so that a direct comparison with data is not possible.

In addition there is a general difficulty with canonical or grand canonical treatments of small systems. In principle all thermostatic information about a system, including the liquid–gas phase transition, is contained in the level

density $\rho(E,N)$ of the Hamiltonian, where E is the energy and N the particle number. When a phase transition occurs $\rho(E,N)$ shows a rapid increase. In a grand canonical (or canonical) ensemble the thermal weight factor is $\rho(E,N)\exp\{-(E-\mu N)/T\}$ (T temperature, μ chemical potential) so that a sudden increase in $\rho(E,N)$ is washed out by the exponential Boltzmann factor. This insensitivity is annoying for small systems because there the level density $\rho(E,N)$ does not raise so steeply with E or N that the product $\rho(E,N)\exp\{-(E-\mu N)/T\}$ forms a very narrow peak as a function of E or N. The micro canonical situation is then preferable as it is directly sensitive to $\rho(E,N)$ within an interval ΔE [7].

Micro canonical statistical models [8, 9] are in this respect well suited but they are static and rely on the assumption that at freeze–out the system is in global equilibrium, both, in chemical and kinetic degrees of freedom.

In the following we investigate the liquid–gas phase transition with a Fermionic Molecular Dynamics simulation. This model can treat nucleus nucleus collisions as well as equilibrium situations. We will however concentrate on an experimentally not feasible situation, namely an excited nucleus which is put in an external field. This field plays the role of a container so that evaporated nucleons cannot escape but equilibrate with the remaining nucleus (hot liquid).

3. Fermionic Molecular Dynamics

This section contains a brief outline of Fermionic Molecular Dynamics (FMD). Details can be found in ref. [10]. The model describes the many–body system with a parameterized antisymmetric many–body state

$$|\,Q(t)\,\rangle = \sum_{all\ P} sign(P)\;|\,q_{P(1)}(t)\,\rangle \otimes \cdots \otimes\; |\,q_{P(A)}(t)\,\rangle \tag{1}$$

composed of single–particle Gaussian wave packets

$$\begin{aligned} \langle\,\vec{x}\,|\,q(t)\,\rangle \;&=\; \exp\left\{-\frac{(\,\vec{x}-\vec{b}(t)\,)^2}{2\,a(t)}\right\}\otimes\;|\,m_s\,\rangle\otimes\;|\,m_t\,\rangle\;, \\ &\vec{b}(t)=\vec{r}(t)+i\,a(t)\,\vec{p}(t)\;, \end{aligned} \tag{2}$$

which are localized in phase space at $\vec{r}$ and $\vec{p}$ with a complex width a. Spin and isospin are chosen to be time–independent in these calculations; they are represented by their z–components m_s and m_t, respectively. Given the Hamilton operator $\underset{\sim}{H}$ the equations of motion for all parameters are derived from the time–dependent variational principle (operators are underlined with a tilde)

$$\delta\int_{t_1}^{t_2} dt\;\langle\,Q(t)\,|\;\;i\frac{d}{dt}-\underset{\sim}{H}\;\;|\,Q(t)\,\rangle \;\;=\;\; 0\;. \tag{3}$$

In the present investigation the effective two–body nucleon–nucleon interaction $\underset{\sim}{V}$ in the Hamilton operator consists of a short–range repulsive and long–range attractive central potential with spin and isospin admixtures and includes the Coulomb potential [11]. The parameters of the interaction have been adjusted to minimize deviations between calculated and measured binding energies for nuclei with mass numbers $4 \leq A \leq 40$.

Besides the kinetic energy $\underset{\sim}{T}$ and the nucleon–nucleon interaction $\underset{\sim}{V}$ the Hamilton operator $\underset{\sim}{H}$ includes an external field

$$\underset{\sim}{U}(\omega) = \frac{1}{2}\, m\omega^2 \sum_{i=1}^{A} \underset{\sim}{\vec{x}}_i^{\,2} \tag{4}$$

which serves as a container.

The container is an important part of the setup because it keeps the evaporated nucleons (vapor) in the vicinity of the remaining liquid drop so that it equilibrates with the surrounding vapor. The vapor pressure is controlled by the external parameter ω, which appoints the accessible volume.

In our model the nuclear system is quantal and strongly interacting. The quantal nature does not allow to deduce the temperature from the kinetic energy distribution as it is the case for classical systems with momentum independent forces. The zero–point motion is always present and does not imply a finite temperature. Due to the fact that the particles are strongly interacting also a fit to a Fermi distribution will give wrong answers because even in the groundstate at zero temperature we have partially occupied single–particle states.

Therefore, the concept of an external thermometer, which is coupled to the nuclear system, is used in the present investigation. The thermometer consists of a quantum system of distinguishable particles moving in a common harmonic oscillator potential different from the container potential.

The time evolution of the whole system is described by the FMD equations of motion. For this purpose the many–body trial state is extended and contains now both, the nucleonic degrees of freedom and the thermometer degrees of freedom

$$|\, Q \,\rangle = |\, Q_n \,\rangle \otimes |\, Q_{th} \,\rangle \; . \tag{5}$$

The total Hamilton operator including the thermometer is given by

$$\underset{\sim}{H} = \underset{\sim}{H}_n + \underset{\sim}{H}_{th} + \underset{\sim}{H}_{n-th} \; , \quad \underset{\sim}{H}_n = \underset{\sim}{T} + \underset{\sim}{V} + \underset{\sim}{U}(\omega) \tag{6}$$

with the nuclear Hamilton operator $\underset{\sim}{H}_n$ and the thermometer Hamilton operator

$$\underset{\sim}{H}_{th} = \sum_{i=1}^{N_{th}} \left(\frac{\vec{\underset{\sim}{k}}^{\,2}(i)}{2\, m_{th}(i)} + \frac{1}{2}\, m_{th}(i)\, \omega_{th}^2\, \vec{\underset{\sim}{x}}^{\,2}(i) \right) \quad . \tag{7}$$

The coupling between nucleons and thermometer particles, $\underset{\sim}{H}_{n-th}$, is chosen to be weak, repulsive and of short range. It has to be as weak as possible in order not to influence the nuclear system too much. On the other hand it has to be strong enough to allow for reasonable equilibration times. Our choice is to put more emphasis on small correlation energies, smaller than the excitation energy, and to tolerate long equilibration times.

The determination of the caloric curve is done in the following way. The nucleus is excited by displacing all wave packets from their ground–state positions randomly. Both, center of mass momentum and total angular momentum are kept fixed at zero. To allow a first equilibration between the wave packets of the nucleus and those of the thermometer the system is evolved over a long time, about 10000 fm/c. (A typical time for a nucleon to cross the hot nucleus is 30 fm/c.) After that a time–averaging of the energy of the nucleonic system as well as of the thermometer is performed over a time interval of 10000 fm/c. During this time interval the mean of the nucleonic excitation energy

$$E \;=\; \frac{1}{N_{steps}} \sum_{i=1}^{N_{steps}} \langle\, Q_n(t_i) \,|\, \underset{\sim}{H}_n \,|\, Q_n(t_i) \,\rangle \tag{8}$$

is evaluated. The time–averaged energy of the thermometer E_{th}, which is calculated during the same time interval, determines the temperature T through the relation for an ideal gas of distinguishable particles in a common harmonic oscillator potential (Boltzmann statistics)

$$T \;=\; \hbar\omega_{th} \left[\ln \left(\frac{E_{th}/N_{th} + \frac{3}{2}\hbar\omega_{th}}{E_{th}/N_{th} - \frac{3}{2}\hbar\omega_{th}} \right) \right]^{-1} \quad . \tag{9}$$

The general idea behind is the assumption of ergodicity; time averaging should be equivalent to ensemble averaging. In an earlier investigation [12] we showed that FMD behaves ergodically. Time averaged occupation numbers of a weakly interacting Fermi gas coincided with a Fermi–Dirac distribution. This however does not mean necessarily that the system as a whole is in a grand canonical ensemble because the one–body occupation numbers represent only a small subset of all degrees of freedom.

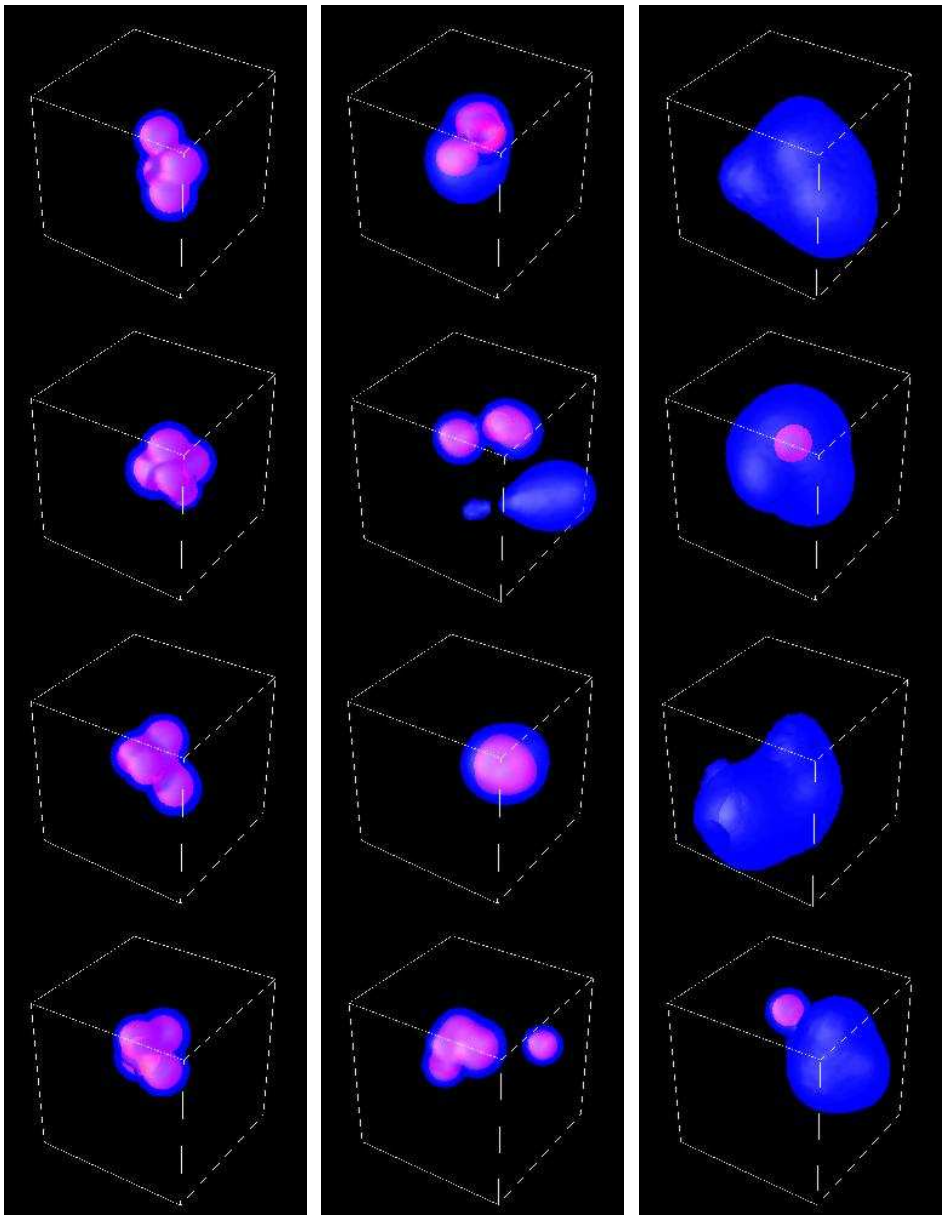

Figure 1. Snapshots of an excited ^{16}O enclosed in a shallow container potential with $\hbar\omega = 1$ MeV and excitation energy per particle of 3.5 MeV (l.h.s.), 7 MeV (center) and 11 MeV (r.h.s.) Bright surfaces enclose densities above $\rho_0/10$ i.e. liquid, darker surfaces $\rho_0/100$ i.e. gas (ρ_0=0.16 fm^{-3} saturation density). The cube is 20 fm each side and drawn to help visualizing three dimensions.

We believe that our system is closer to the micro canonical situation in the sense that the particle number is fixed and a pure many–body state $|\, Q_n(t)\,\rangle$ is evolved in time. This excited state is not an eigenstate of the Hamiltonian but has a certain width in energy. (If it were an eigenstate it would be stationary and there would be no dynamical evolution as seen in Fig 1.) In principle we could calculate the variance $\langle\, Q_n(t)\,|\, \underset{\sim}{H}^2_n \,|\, Q_n(t)\,\rangle - \langle\, Q_n(t)\,|\, \underset{\sim}{H}_n \,|\, Q_n(t)\,\rangle^2$ of the Hamiltonian as a function of time to check our conjecture. But $\underset{\sim}{H}^2_n$ contains a 4–body operator which means a huge numerical effort. The coupling to the thermometer also introduces a certain amount of energy fluctuations but they remain rather small as shown in the following section.

4. Caloric Curves

In Fig. 1 several snap shots of the one–body density of a hot nuclear system with 8 neutrons and 8 protons are shown. On the left hand side the ^{16}O nucleus has been given an excitation energy per particle of 3.5 MeV by randomly displacing the wave packets of the ground state. After equilibration this corresponds to a temperature of about 4 MeV. One sees that the two–body interaction yields an alpha–particle substructure in ^{16}O. There is no gas around the vibrating nucleus because the excitation energy is not high enough to evaporate particles.

In the center column of Fig. 1 the excitation energy is 7 AMeV. Bright areas which indicate the liquid are surrounded by a cloud of gas (for details see figure caption). More over, the nuclear system very often falls apart into several smaller drops which are embedded in vapor.

The right hand side displays the same system but for an excitation energy of 11 AMeV. Here half of the time no high density areas are visible (first and third frame) and if a drop is formed it is rather small.

As we shall see later, the two excitation energies 7 and 11 AMeV correspond both to a temperature around 6 MeV in the coexistence region. It is quite obvious that the additional excitation energy of 4 MeV per particle is used to transform liquid to vapor so that we see a clear first order liquid–gas phase transition. This is remarkable as we are dealing with only 16 nucleons and the dynamical model evolves in time a pure state with a very limited number of degrees of freedom, actually only eight per particle, three for mean position, three for mean momentum and two for the width. Furthermore, we have a fermion system in which the level density due to antisymmetrization is much smaller than in classical mechanics.

The container is very wide so that the vapor pressure is rather small. Estimates yield 10^{-4} to 10^{-2} MeV/fm^3 which should be compared to a

critical pressure of about 0.5 MeV/fm^3. The container potential itself is at the surface of the indicated cubes only 1.2 MeV higher than in the center.

To quantify the relation between energy, temperature and container size we display in Fig. 2 the caloric curve for the external parameter $\hbar\omega$ = 1, 6 and 18 MeV, which controls the thermodynamic properties of the nucleonic system in a similar way as the volume. A pronounced plateau is seen in the plot on the left hand side, where the oscillator does not influence the self–bound nucleus very much. In the middle part the more narrow container potential is already squeezing the ground state, its energy goes up to $E/A \approx -5$ MeV. The plateau is shifted to $T \approx 7$ MeV and the latent heat is decreased. On the right hand side, for $\hbar\omega = 18$ MeV, the coexistence region has almost vanished and the critical temperature T_c is reached.

The solid line represents the relation between temperature and energy for an ideal Fermi gas in a harmonic oscillator potential with $\omega_{\rm eff} = (\omega^2 + \omega_0^2)^{1/2}$, where $\hbar\omega_0 = 10$ MeV corresponds to the selfconsistent mean–field of ^{16}O. The energy zero–point is shifted so that the ground state of the oscillator is at the FMD value. The dashed line shows the relation for the external container, also with the ground state shifted, because even in the gas phase the particles still feel attraction. Despite the strong interaction the liquid and the gas phase follow approximately the picture of an ideal gas in a mean–field. The coexistence region cannot be approximated by a mean–field picture like the liquid in a selfconsistent potential or the gas in the external field.

The "error bars" in temperature and energy represent r.m.s. deviations from the time averaged mean. There is always an exchange of energy between thermometer and nuclear system. But the fluctuations remain rather small. The temperature fluctuations, which through relation (9) are actually fluctuations in the energy of the thermometer particles, are larger because the thermometer has a smaller heat capacity than the nucleons.

The critical temperature T_c can only be estimated from the disappearance of the coexistence phase in Fig. 2 because the fluctuations in T and E are rather large. Its value is about 10 MeV and has to be compared to the results of ref. [2, 4, 16] for finite nuclei including Coulomb and surface effects. All authors report a week dependence of the critical temperature on the mass number in the region from calcium to lead. The result of Jaqaman et al. with the Skyrme ZR3 interaction [2] can be extrapolated to ^{16}O to give $T_c \approx 8$ MeV, Bonche et al. [4] arrive at the same number using the SKM interaction, but got $T_c \approx 11$ MeV with the SIII interaction. Close to the last result is the value extrapolated from ref. [16] where $T_c \approx 11.5$ MeV for Gogny's D1 interaction.

We determined the relation between the excitation energy and the tem-

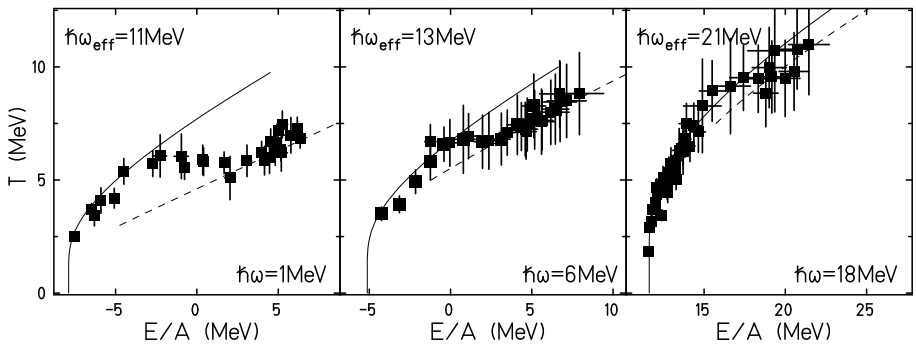

Figure 2. Caloric curve of ^{16}O for the frequencies $\hbar\omega = 1, 6, 18$ MeV of the container potential. The solid lines show the low temperature behaviour of an ideal gas of 16 fermions in a common harmonic oscillator with level spacing $\hbar\omega_{\rm eff}$, the dashed lines denote their high temperature behaviour in the confining oscillator ($\hbar\omega$).

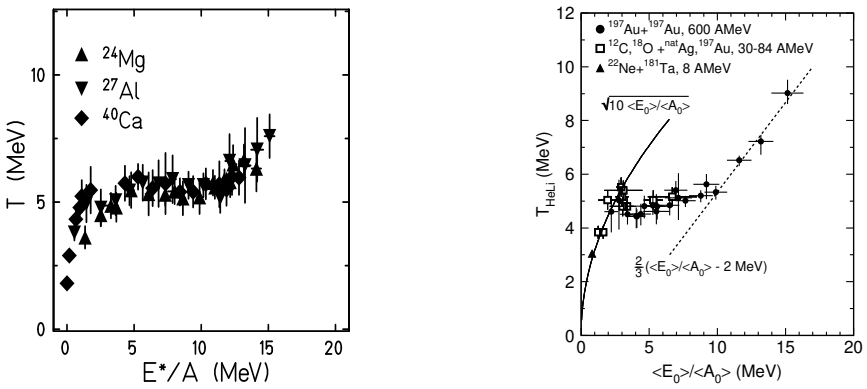

Figure 3. L.h.s.: caloric curve of ^{24}Mg, ^{27}Al and ^{40}Ca at $\hbar\omega = 1$ MeV, r.h.s.: caloric curve determined by the Aladin group from the decay of spectator nuclei.

perature also for the larger nuclei ^{24}Mg, ^{27}Al and ^{40}Ca using the same container potential with $\hbar\omega = 1$ MeV and summarize them on the left hand side of Fig. 3. In order to put them on the same scale we subtract from the averaged energy, defined in eq. (8), the respective ground state energies and show the temperature as a function of excitation energy E^*.

Like for ^{16}O all caloric curves clearly exhibit three different parts. Beginning at small excitation energies the temperature rises steeply with increasing energy as expected for the shell model. The nucleons remain bound in the excited nucleus which behaves like a drop of liquid. At an excitation energy of 3 MeV per nucleon the curve flattens and stays almost constant up to about 11 MeV. This coexistence plateau at $T \approx 5$ to 6 MeV reaches

from $E^*/A \approx 3$ MeV to about $E^*/A \approx 11$ MeV where all nucleons are unbound and the system has reached the vapor phase. The latent heat at pressure close to zero is hence about 8 MeV.

One has to keep in mind that the plateau, which due to finite size effects is rounded, is not the result of a Maxwell construction as in nuclear matter calculations. In the excitation energy range between 3 and 11 MeV per particle an increasing number of nucleons is found in the vapor phase outside the liquid phase. This has been shown in Fig. 1.

The caloric curve shown in Fig. 3 has a striking similarity with the caloric curve determined by the ALADIN group [13] which is displayed in the same figure. The position and the extension of the plateau agree with the FMD calculation using a containing oscillator potential of $\hbar\omega = 1$ MeV. Nevertheless, there are important differences. The measurement addresses an expanding non–equilibrium system, but the calculation deals with a contained equilibrium system. In addition the used thermometers differ; the experiment employs an isotope thermometer based on chemical equilibrium and the calculation uses an ideal gas thermometer. One explanation why the thermodynamic description of the experimental situation works and compares nicely to the equilibrium result might be, that the excited spectator matter equilibrates faster into the coexistence region [15] than it expands and cools. The assumption of such a transient equilibrium situation [14, 8, 9] seems to work rather well at least in the plateau region.

References

1. see the different contributions in these proceedings and the references therein
2. H.R. Jaqaman, A.Z. Mekjian, L. Zamik, Phys. Rev. C **29** (1984) 2067
3. A.L. Goodman, J.I. Kapusta, A.Z. Mekjian, Phys. Rev. C **30** (1984) 851
4. P. Bonche, S. Levit, D. Vautherin, Nucl. Phys. **A427** (1984) 278 and Nucl. Phys. **A436** (1985) 265
5. B. Serot, J.D. Walecka, Adv. Nucl. Phys. **16** (1986)
6. M. Schönhofen et al., Nucl. Phys. **A504** (1989) 875
7. see for example the contribution of A. Hüller and D.H.E. Gross in these proceedings
8. J.P. Bondorf, R. Donagelo, I.N. Mishustin, C.J. Pethick, H. Schulz, K. Sneppen, Nucl. Phys. **A443** (1985) 321
9. D.H.E. Gross, Rep. Prog. Phys. **53** (1990) 605; Pys. Rep. **279** (1997) 119
10. H. Feldmeier, Nucl. Phys. **A515** (1990) 147; H. Feldmeier, K. Bieler, J. Schnack, Nucl. Phys. **A586** (1995) 493; H. Feldmeier, J. Schnack, Nucl. Phys. **A583** (1995) 347; H. Feldmeier, J. Schnack, Prog. Part. Nucl. Phys. **39** (1997)
11. J. Schnack, PhD thesis, TH Darmstadt (1996)
12. J. Schnack, H. Feldmeier, Nucl. Phys. **A601** (1996) 181
13. J. Pochodzalla et al., Phys. Rev. Lett. **75** (1995) 1040; Prog. Part. Nucl. Phys. 39(1997)443
14. G. Papp, W. Nörenberg, APH Heavy Ion Physics 1 (1995) 241
15. H. Feldmeier, J. Schnack, Advances in Nuclear Dynamics 3, Proc. 13th Winter Workshop on Nuclear Dynamics, p.83, eds: W. Bauer and A. Mignerey, Plenum Press (1997), ISBN 0-306-45719-9
16. Fu-guang Cao, Shan-de Yang, preprint, nucl-th/9612022